Interaction of Cr(diimine)$_3^{3+}$ Complexes with DNA†

Rhett T. Watson, Nehal Desai, Justin Wildsmith, John F. Wheeler,* and Noel A. P. Kane-Maguire*

Department of Chemistry, Furman University, Greenville, South Carolina 29613-1120

Received July 21, 1998

Luminescence spectroscopy coupled with capillary electrophoresis (CE) provides insight into the nature and stereoselectivity of Cr(diimine)$_3^{3+}$ interactions with polynucleotides. Photoluminescence measurements on Cr(phen)$_3^{3+}$ and Cr(bpy)$_3^{3+}$ in air or N_2-saturated solution demonstrate strong B-DNA quenching of Cr(diimine)$_3^{3+}$ emission intensities and lifetimes. Both dynamic and static quenching are observed, the latter being attributed to DNA bound Cr(diimine)$_3^{3+}$. Very rapid quenching is also observed with deoxyguanosine monophosphate (dGMP), while no bimolecular quenching is observed with other mononucleotides. Likewise, poly(dG-dC)·poly(dG-dC) causes rapid quenching, while only minor quenching is observed for poly(dA-dT)·poly(dA-dT). These emission results are consistent with a DNA quenching mechanism involving guanine base oxidation. The electropherogram resulting from the co-injection of *rac*-Cr(phen)$_3^{3+}$ and *rac*-Ru(phen)$_3^{2+}$ into a capillary containing B-DNA indicates a similar binding constant for the two complexes, while the enantiomeric stereoselectivities are reversed. CE studies for Ru(phen)$_3^{2+}$ with distamycin A (an AT selective minor groove binder) reveal a significant reduction in complex migration times *and* a complete loss of enantiomeric discrimination. These results are consistent with a literature model where nonelectrostatic binding for both isomers occurs in the *minor* groove. Analogous distamycin studies with Cr(phen)$_3^{3+}$ are also in accord with minor groove binding.

Introduction

The last two decades have witnessed the emergence of a rich chemistry associated with the interaction of chiral transition metal (TM) complexes with DNA. The most widely investigated systems have been Ru(diimine)$_3^{2+}$ compounds, where the room temperature (RT) emission signal has proven a valuable probe of DNA binding.[1] However, with several notable exceptions,[2] the lowest-lying ^{3}MLCT excited states of these Ru^{2+} complexes are incapable of causing a *direct* one electron oxidation of guanine (the most easily oxidized nucleobase).[3] In contrast, Rh^{3+} complexes containing 9,10-phenanthrenequinone diimine (phi) ligands have an E° ($^*Rh^{3+}/Rh^{2+}$) value ≈+2 V versus NHE,[4] and these systems cause *direct* (frank) DNA photocleavage via deoxyribose oxidation.[5] However, the absence of a RT luminescence signature has limited their application as DNA reporters. Cr(diimine)$_3^{3+}$ complexes would appear to combine several of the attractive features of both the Ru^{2+} and Rh^{3+} systems, in view of their long-lived RT emission and strong excited-state oxidizing power.[6] We have recently proposed that CE may provide a rapid screening method for determining both relative binding constants and stereoselectivities of TM interactions with DNA.[7] In this report we demonstrate that luminescence spectroscopy coupled with capillary electrophoresis (CE) studies provides important insight into the nature and stereoselectivity of Cr(diimine)$_3^{3+}$ interactions with polynucleotides.

Experimental Section

Chemicals. Racemic PF_6^- and $CF_3SO_3^-$ salts of Ru(phen)$_3^{2+}$ were obtained by metathesis from the commercially available Cl^- salt (Aldrich). PF_6^- salts of Λ-Ru(phen)$_3^{2+}$ and Δ-Ru(phen)$_3^{2+}$ were isolated via a slight modification of the literature method.[8] For all Ru(phen)$_3^{2+}$ solutions, concentrations were determined by using a molar absorptivity value of $\epsilon_{446} = 19\,000\ M^{-1}\ cm^{-1}$.[9] The synthesis of racemic [Cr(phen)$_3$](PF$_6$)$_3$, [Cr(bpy)$_3$](PF$_6$)$_3$, and [Cr(TMP)$_3$](CH$_3$COO)$_3$ (where TMP = 3,4,7,8- tetramethyl-1,10-phenanthroline) followed closely the procedure described by Kane-Maguire and Hallock.[10] Optically active PF_6^- salts of Cr(phen)$_3^{3+}$ were obtained via a literature method.[11] Concentrations of Cr(phen)$_3^{3+}$, Cr(bpy)$_3^{3+}$, and Cr(TMP)$_3^{3+}$ solutions were calculated using molar absorptivity values of $\epsilon_{354} = 4200\ M^{-1}\ cm^{-1}$, $\epsilon_{344} = 7400\ M^{-1}\ cm^{-1}$, and $\epsilon_{320} = 12\,300\ M^{-1}\ cm^{-1}$, respectively. Calf thymus B-DNA was purchased from Sigma ($\epsilon_{258} = 6600\ M^{-1}\ cm^{-1}$),[12] while the synthetic polynucleotides poly(dA-dT)·poly(dA-dT) and poly(dG-dC)·poly(dG-dC) were obtained from Pharmacia LKB Biotechnology Inc ($\epsilon_{262} = 6600\ M^{-1}\ cm^{-1}$ and $\epsilon_{253} = 7400\ M^{-1}\ cm^{-1}$, respectively).[12]

* To whom correspondence should be addressed. Tel.: (864) 294-3374; (864) 294-3371. Fax: (864) 294-3559. E-mail: noel.kane-maguire@furman.edu; john.wheeler@furman.edu.

† Presented in part at the 216th National Meeting of the American Chemical Society, Boston, MA, August 23−27, 1998 (Paper 118).

(1) (a) Turro, N. J.; Barton, J. K.; Tomalia, D. A. *Acc. Chem. Res.* **1991**, *24*, 332−340. (b) Holmlin, R. E.; Stemp, E. D. A.; Barton, J. K. *Inorg. Chem.* **1998**, *37*, 29−34.
(2) (a) Kirsch-De Mesmaeker, A.; Orellana, G.; Barton, J. K.; Turro, N. J. *Photochem. Photobiol.* **1990**, *52*, 461−472. (b) Lecomte, J.-P.; Kirsch-De Mesmaeker, A.; Feeney, M. M.; Kelly, J. M. *Inorg. Chem.* **1995**, *34*, 6481−6491.
(3) Burrows, C. J.; Muller, J. G. *Chem. Rev.* **1998**, *98*, 1109−1151.
(4) Turro, C.; Evenzahav, A.; Bossmann, S. H.; Barton, J. K.; Turro, N. J. *Inorg. Chim. Acta* **1996**, *243*, 101−108.
(5) (a) Terbrueggen, R. H.; Barton, J. K. *Biochemistry* **1995**, *34*, 8227−8234. (b) Armitage, B. *Chem. Rev.* **1998**, *98*, 1171−1200.
(6) Jamieson, M. A.; Serpone, N.; Hoffman, M. Z. *Coord. Chem. Rev.* **1981**, *39*, 121.
(7) Shelton, C. M.; Seaver, K. E.; Wheeler, J. F.; Kane-Maguire, N. A. P. *Inorg. Chem.* **1997**, *36*, 1532−1533.
(8) Dwyer, F. P.; Gyarfas, E. C. *J. Proc. R. Soc. N. S. W.* **1949**, *83*, 170−173.
(9) Lin, C. T.; Boettcher, W.; Chou, M.; Creutz, C.; Sutin, N. *J. Am. Chem. Soc.* **1976**, *98*, 6536−6544.
(10) Kane-Maguire, N. A. P.; Hallock, J. S. *Inorg. Chim. Acta* **1979**, *35*, L309−L311.
(11) Lee, C. S.; Gorton, E. M.; Neumann, H. M.; Hunt, H. R. *Inorg. Chem.* **1966**, *5*, 1397−1399.
(12) Barton, J. K.; Goldberg, J. M.; Kumar, C. V.; Turro, N. J. *J. Am. Chem. Soc.* **1986**, *108*, 2081−2088.

10.1021/ic980857l CCC: $18.00
Published on Web 05/11/1999

The mononucleotides 2′-deoxyguanosine-5′-monophosphate disodium salt hydrate (dGMP), 2′-deoxyadenosine-5′-monophosphoric acid monohydrate (dAMP), and 2′-deoxycytidine-5′-monophosphoric acid monohydrate (dCMP) were used as received from Aldrich, while thymidine-5′-monophosphate sodium salt and distamycin A hydrochloride were purchased from Sigma. Distamycin concentrations were obtained by utilizing a molar absorptivity value of $\epsilon_{302} = 37\,000\ M^{-1}\ cm^{-1}$.[1b]

Instrumentation and Methods. Electronic absorption spectra were recorded on a HP8452A diode array spectrophotometer, while a JASCO 710 spectropolarimeter was employed for circular dichroism (CD) measurements. An SLM 8000C spectrofluorimeter employing a red sensitive Hamamatsu R928 photomultiplier tube was used to record steady-state emission spectra. For excited-state lifetime measurements, pulse excitation was performed with a N_2/dye laser system (Molectron UV-12/Molectron DL-14) using either the 337 nm N_2 line or the 440 nm line obtained by using a coumarin 120 dye. Emission was detected at right angles via a J-Y Optics H10V monochromator, a CS3−71 cutoff filter, and a Hamamatsu R928 photomultiplier tube. Emission signals were fed via the appropriate load resistor into a LeCroy 9350A 500 MHz digital oscilloscope. Lifetimes were obtained by first-order kinetic analysis of the phosphorescence signals using the VuPoint 3 program developed by Ventura Publishers (Maxwell Technologies, Inc).

Capillary electrophoresis (CE) studies were carried out using a Beckman Instruments P/ACE 5000 HPCE system with UV−vis detection. Additional 1.00 cm absorbance filters for measurements at $\lambda > 300$ nm were purchased from Corion. Uncoated fused silica capillary (50 μm i.d. × 363 μm o.d.) was obtained from Polymicro Technologies and treated with 1.0 M NaOH prior to use. In experiments where the contribution of electroosmotic flow was determined, free 1,10-phenanthroline was used as a neutral marker. Coated capillaries were prepared using the modified linear acrylamide procedure of Sepaniak, et al. and were stored in 10 mM H_3PO_4.[13] CE buffers were prepared from HPLC-purity Tris-HCl titrated with NaOH. DNA and DNA/distamycin solutions were freshly prepared for experiments by stirring or brief sonication in Tris-HCl/NaCl followed by dilution with doubly deionized water.

Results and Discussion

$Cr(phen)_3^{3+}$ Emission Quenching by B-DNA. Photoluminescence studies on $Cr(phen)_3^{3+}$ in air or N_2-saturated 50 mM Tris-HCl buffer (pH 7.1) solutions in the presence and absence of B-DNA reveal strong polynucleotide quenching of the steady-state $^2E_g \rightarrow {}^4A_{2g}$ (O_h) phosphorescence signal at 730 nm[14] and the corresponding emission lifetime. A typical example of steady-state emission signal quenching by B-DNA under air-saturated conditions is shown in Figure 1. This behavior is in marked contrast to that normally observed for $Ru(diimine)_3^{2+}$ systems, which are characterized by increases (sometimes dramatic) in the emission intensity upon DNA binding.[15,16] Representative steady-state emission intensity and lifetime Stern−Volmer plots for quenching of *rac*-$Cr(phen)_3^{3+}$ phosphorescence by calf thymus B-DNA in *air-saturated* solution (22 °C) are shown in Figure 2. A good straight line fit is apparent for the SV plot of the lifetime data, in accord with *dynamic* quenching by DNA of the ^2E_g excited state (i.e. collisional deactivation). Dividing the SV slope by the lifetime in the absence of DNA yields a bimolecular quenching rate constant of $1.1 \times 10^8\ M^{-1}\ s^{-1}$. The corresponding SV plot of the emission intensity, however, shows strong upward curvature at higher DNA concentrations. Such behavior is diagnostic of

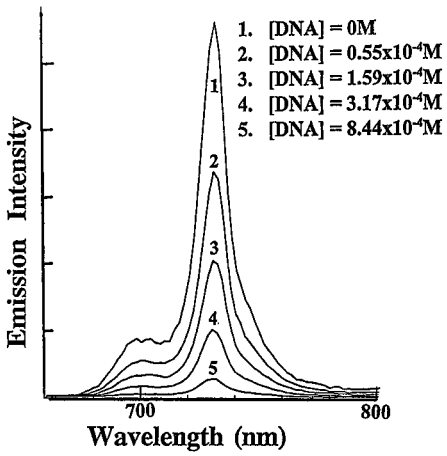

Figure 1. Steady-state emission spectrum of an air-saturated 3.3×10^{-5} M solution of *rac*-$Cr(phen)_3^{3+}$ in 50 mM Tris-HCl buffer (pH 7.1) in the presence of different concentrations of calf thymus B-DNA (wavelength of excitation = 320 nm).

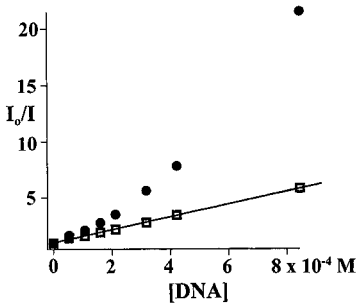

Figure 2. Stern−Volmer plots for emission quenching of an air-saturated 3.3×10^{-5} M solution of *rac*-$Cr(phen)_3^{3+}$ in 50 mM Tris-HCl buffer (pH 7.1) by calf thymus B-DNA: (●) steady-state emission intensity data, $I_o/I = \Phi_o/\Phi$ ($\lambda_{exc} = 320$ nm); (□) emission lifetime data, $I_o/I = \tau_o/\tau$ (temp: 22 °C).

an additional deactivation pathway involving *static* quenching[17]—attributed in this case to DNA bound $Cr(phen)_3^{3+}$, which constitutes a nonluminescent association pair. It is noteworthy that pulsed emission decays followed strict first-order kinetics, consistent with the absence of detectable emission from $Cr(phen)_3^{3+}$ bound to DNA. It can be shown[17] that when both dynamic and static quenching are present

$$\text{SV Slope}_{SS} = (\text{SV Slope}_\tau + \beta K_{DNA}) + \text{SV Slope}_\tau\,(\beta K_{DNA})[\text{DNA}] \quad (1)$$

where SV Slope_{SS} and SV Slope_τ are the experimental slopes of the Stern−Volmer emission intensity and lifetime plots, K_{DNA} is the $Cr(phen)_3^{3+}$/DNA binding constant, and $\beta = 1$ under our experimental conditions. At *low* [DNA], eq 1 reduces to

$$\text{SV Slope}_{SS} = \text{SV Slope}_\tau + \beta K_{DNA} \quad (2)$$

Thus a binding constant value of $K_{DNA} = 3500\ M^{-1}$ for *rac*-$Cr(phen)_3^{3+}$ may be estimated from the differences in the emission intensity and lifetime SV slopes at low [DNA]. Reported K_{DNA} values for $Ru(phen)_3^{2+}$ are comparable under reasonably similar conditions,[18] consistent with the CE data presented below. Emission data for the $Cr(phen)_3^{3+}$/B-DNA system are also amenable to Scatchard plot analysis, where a

(13) Stebbins, M. A.; Schar, C. R.; Peterson, C. B.; Sepaniak, M. J. *J. Chromatogr. B* **1997**, *697*, 181−188.
(14) Kane-Maguire, N. A. P.; Langford, C. H. *J. Chem. Soc., Chem. Commun.* **1971**, 895−896.
(15) Pyle, A. M.; Rehmann, J. P.; Meshoyrer, R.; Kumar, C. V.; Turro, N. J.; Barton, J. K. *J. Am. Chem. Soc.* **1989**, *111*, 3051−3058.
(16) Hartshorn, R. M.; Barton, J. K. *J. Am. Chem. Soc.* **1992**, *114*, 5919−5925.
(17) Demas, J. N.; Addington, J. W. *J. Am. Chem. Soc.* **1974**, *96*, 3663−3664.
(18) Kalsbeck, W. A.; Thorp, H. H. *J. Am. Chem. Soc.* **1993**, *115*, 7146−7151.

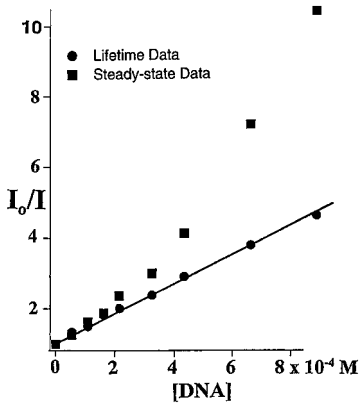

Figure 3. Stern−Volmer plots for emission quenching of an air-saturated 3.1×10^{-5} M solution of *rac*-Cr(bpy)$_3^{3+}$ in 50 mM Tris-HCl buffer (pH 7.1) by calf thymus B-DNA: (■) steady-state emission intensity data, $I_o/I = \Phi_o/\Phi$ ($\lambda_{exc} = 320$ nm); (●) emission lifetime data, $I_o/I = \tau_o/\tau$ (temp: 22 °C).

data fit to the McGhee and von Hippel equation appropriate for noncooperative binding[15,19] yields a K_{DNA} value of 4000 M^{-1} and a binding ratio of 0.6 Cr(phen)$_3^{3+}$ per DNA base pair. Finally, it is noted that an identical value for the bimolecular rate constant for quenching of Cr(phen)$_3^{3+}$ emission by B-DNA is observed under *N_2-purged* solution conditions, indicating the absence of a key role for oxygen in the quenching process.

Cr(bpy)$_3^{3+}$ Emission Quenching by B-DNA. A more restricted study was done on the *rac*-Cr(bpy)$_3^{3+}$ system. Steady-state emission intensity and lifetime Stern−Volmer plots are shown in Figure 3 for air-saturated conditions. As previously noted for the phenanthroline analogue, upward curvature is observed in the emission intensity plot at higher DNA concentrations, and is attributed again to *static* (association pair) quenching. The upward curvature is not as marked as in the Cr(phen)$_3^{3+}$ case, and is suggestive of a smaller DNA binding constant (smaller binding constants for bpy species have been previously noted for Ru(diimine)$_3^{2+}$ systems).[15,18] The SV plot of the *rac*-Cr(bpy)$_3^{3+}$ lifetime data exhibits a good straight line fit, consistent with the presence of a bimolecular quenching component. When the experimental lifetime slope is divided by the emission lifetime in the absence of B-DNA, a bimolecular quenching rate constant of 1.0×10^8 M^{-1} s^{-1} is obtained (i.e., a value esssentially identical to that noted above for Cr(phen)$_3^{3+}$).

Mechanism of Emission Quenching. Several different lines of evidence suggest that Cr(phen)$_3^{3+}$ and Cr(bpy)$_3^{3+}$ emission quenching by B-DNA proceeds via an *electron transfer* mechanism involving guanine base oxidation. The ^2E_g excited states of Cr(phen)$_3^{3+}$ and Cr(bpy)$_3^{3+}$ have been previously employed as photooxidants for a wide range of nonbiological substrates, and have an oxidizing power of +1.4 V versus NHE.[6] Therefore, they are thermodynamically capable of oxidizing guanine in DNA ($E°_{G,G+}$, pH 7 ≈ −1.2 V versus NHE), while oxidation of the other DNA bases is improbable.[3] The results of emission quenching studies by mononucleotides and several synthetic polynucleotides (see below) are consistent with these expectations.

Emission Quenching by Mononucleotides. (a) Quenching by dGMP. We observe that deoxyguanosine-5′-monophosphate (dGMP) rapidly quenches *rac*-Cr(phen)$_3^{3+}$ emission (both intensity and lifetime) in air-saturated solution. Interestingly, in this case the intensity and lifetime SV quenching plots are collinear (Figure 4). The absence of a significant static quenching component may reflect a smaller ion-pair formation constant than that for Cr(phen)$_3^{3+}$/B-DNA. However, an additional factor is undoubtedly the 20-fold increase in the bimolecular quenching rate constant, k_q, which results in the data being collected over a much smaller range of quencher concentrations. The observed k_q value of 2.2×10^9 M^{-1} s^{-1} is very close to the diffusion controlled value reported for GMP quenching of the emission of Ru(II) complexes containing strongly oxidizing ligands such as HAT and TAP (for which oxidation of the nucleobase guanine has been conclusively demonstrated).[2]

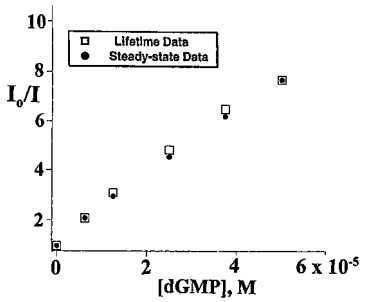

Figure 4. Stern−Volmer plots for emission quenching of an air-saturated 3.2×10^{-5} M solution of *rac*-Cr(phen)$_3^{3+}$ by deoxyguanosine-5′-monophosphate (dGMP) in 50 mM Tris-HCl buffer (pH 7.1): (●) steady-state emission intensity data, $I_o/I = \Phi_o/\Phi$ ($\lambda_{exc} = 320$ nm); (□) emission lifetime data, $I_o/I = \tau_o/\tau$ (temp: 22 °C).

In addition, we have investigated emission quenching by dGMP for the complex *rac*-Cr(TMP)$_3^{3+}$ (where TMP is 3,4,7,8-tetramethyl-1,10-phenanthroline). This complex has an $E°$ (*Cr^{3+}/Cr^{2+}) value of +1.1V[20] compared with the +1.4 V value for Cr(phen)$_3^{3+}$, and thus should only be marginally capable of oxidizing a guanine nucleobase. This expectation is in accord with the markedly different quenching behavior observed for the Cr(TMP)$_3^{3+}$ complex. At a dGMP concentration of 2.6×10^{-4} M (i.e., five times the highest concentration in the Cr(phen)$_3^{3+}$ study) no quenching is observed within experimental error in the steady-state emission signal of the Cr(TMP)$_3^{3+}$ species. This observation is indicative of a very minor role for electron-transfer quenching in the Cr(TMP)$_3^{3+}$ system.

(b) Quenching by dAMP, dCMP, and dTMP. In striking contrast to the dGMP results for Cr(phen)$_3^{3+}$, the less readily oxidizable adenosine (dAMP), cytosine (dCMP), and thymidine (dTMP) mononucleotides demonstrate no *bimolecular* quenching of Cr(phen)$_3^{3+}$ emission. In Figure 5 the emission lifetimes of Cr(phen)$_3^{3+}$ are plotted versus mononucleotide concentration. Although some decrease in emission lifetime is apparent for dAMP, dCMP, and dTMP, the absence of bimolecular quenching is evident from the *limiting* lifetime value reached as the nucleotide concentration is increased. We attribute this limiting value to the intrinsic lifetime of the Cr(phen)$_3^{3+}$/mononucleotide ion-pair species. These observations also provide evidence against an alternative redox quenching mechanism involving the deoxyribosyl units.

Emission Quenching by Synthetic Polynucleotides. Further support for a quenching mechanism involving direct guanine base oxidation comes from analogous studies on Cr(phen)$_3^{3+}$ with synthetic polynucleotides. The duplex poly(dG-dC)·poly(dG-dC) yields similar quenching data (Figure 6) to that noted earlier for B-DNA (Figure 2), with clear evidence for ion-pair

(19) Concentrations of unbound Cr(phen)$_3^{3+}$ needed for such plots were obtained from the pulsed emission intensity, I_o, at different [DNA], after extrapolation to zero time after the pulse. i.e., $[Cr(phen)_3^{3+}]_{free}$ = (I_o with DNA/I_o no DNA) $[Cr(phen)_3^{3+}]_{total}$.

(20) Serpone, N.; Jamieson, M. A.; Emmi, S.; Fuochi, P. G.; Mulazzani, Q. G.; Hoffman, M. Z. *J. Am. Chem. Soc.* **1981**, *103*, 1091−1098.

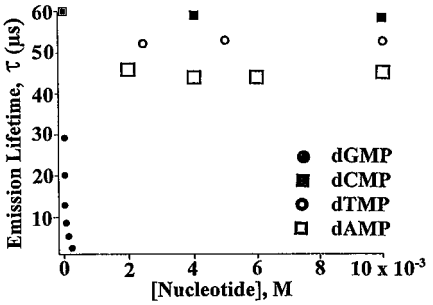

Figure 5. Dependence of the emission lifetime of *rac*-$Cr(phen)_3^{3+}$ (3.3×10^{-5} M) in an air-saturated 50 mM Tris-HCl buffer solution (pH 7.1) on mononucleotide concentration for the mononucleotides dGMP, dAMP, dCMP, and dTMP (temp: 22 °C).

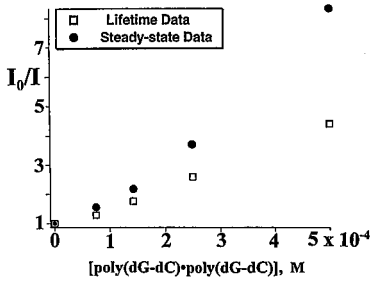

Figure 6. Stern−Volmer plots for emission quenching of an air-saturated 3.2×10^{-5} M solution of *rac*-$Cr(phen)_3^{3+}$ in 50 mM Tris-HCl buffer (pH 7.1) by poly(dG-dC)•poly(dG-dC): (●) steady-state emission intensity data, $I_o/I = \Phi_o/\Phi$ (λ_{exc} = 320 nm); (□) emission lifetime data, $I_o/I = \tau_o/\tau$ (temp: 22 °C).

Table 1. Emission Intensities and Lifetimes of $Cr(phen)_3^{3+}$ (3.4×10^{-5} M) in the Presence of Poly(dA-dT)•Poly(dA-dT) in Air-Saturated 50 mM Tris-HCl Buffer, pH 7.1 (Temp: 22 °C)

[poly(dA-dT)•poly(dA-dT)]	relative Φ_{320}[a]	lifetime, τ (μs)
0 M	1.00	62
0.91×10^{-4} M	0.93	58
5.1×10^{-4} M	0.60	44
9.1×10^{-4} M	0.58	42

[a] Φ_{320} = relative steady-state emission intensity on 320 nm excitation.

(static) quenching at higher nucleotide concentrations and a bimolecular quenching rate constant of 1.1×10^8 M^{-1} s^{-1}. However, in the presence of poly(dA-dT)•poly(dA-dT) only a minor reduction occurs in emission intensities and lifetimes (see Table 1), both of which approach a limiting value at higher [nucleotide] values. Such behavior is inconsistent with a significant role for electron-transfer quenching, and is attributed to a somewhat lower emission efficiency and lifetime for the ion-paired $Cr(phen)_3^{3+}$ complex.

Specificity of Base Sequence Binding. The $Cr(phen)_3^{3+}$ emission signal in the presence of two different polynucleotides may provide useful information on the relative binding constants. A comparison of *rac*-$Cr(phen)_3^{3+}$ steady-state emission intensity and lifetime data at low loadings of Cr/polynucleotide for a 1:1 mixture of poly(dA-dT)•poly(dA-dT) and poly(dG-dC)•poly(dG-dC) with those for solutions containing only a single polynucleotide is provided in Table 2. At low Cr/nucleotide loadings, quenching by *both* nucleotides should be primarily associated with ion-pair formation (since under these conditions static quenching is dominant for poly(dG-dC)•poly(dG-dC)—see Figure 6). The emission intensities and lifetimes shown in Table 2 for $Cr(phen)_3^{3+}$ in mixed polynucleotide solutions are considerably closer to those characteristic of solutions containing only poly(dA-dT)•poly(dA-dT), which suggests a significant AT binding preference for $Cr(phen)_3^{3+}$.

Table 2. Emission Intensities and Lifetimes of $Cr(phen)_3^{3+}$ (6.0×10^{-5} M) in the Presence of Poly(dA-dT)•Poly(dA-dT) and/or Poly(dG-dC)•Poly(dG-dC) in Air-Saturated 50 mM Tris-HCl Buffer, pH 7.1 (Temp: 22 °C)

[polynucleotide]	relative Φ_{320}[a]	lifetime, τ (μs)
0 M	1.00	62
1.0×10^{-3} M GC[b]	0.10	13
2.0×10^{-3} M GC	0.03	9
1.0×10^{-3} M AT[c]	0.73	52
2.0×10^{-3} M AT	0.63	46
1.0×10^{-3} M GC/ 1.0×10^{-3} M AT	0.39	42

[a] Φ_{320} = relative steady-state emission intensity on 320 nm excitation. [b] GC = poly(dG-dC)•poly(dG-dC). [c] AT = poly(dA-dT)•poly(dA-dT).

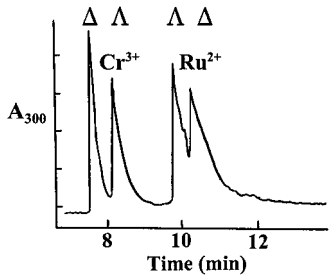

Figure 7. Electropherogram of a 1:1 mixture of *rac*-$Cr(phen)_3^{3+}$ and *rac*-$Ru(phen)_3^{2+}$ (0.8 mM) in 50 mM Tris-HCl buffer, pH 7.4, containing 100 mM NaCl and 3 mM calf-thymus B-DNA. Electrophoretic field strength was 260 V/cm (50 μm i.d. *uncoated* capillary), using a run temperature of 35 °C. Detection was at λ = 300 nm.

Capillary Electrophoresis Studies. Figure 7 shows the resultant electropherogram when a 1:1 mixture of *rac*-$Cr(phen)_3^{3+}$ and *rac*-$Ru(phen)_3^{2+}$ was injected into a capillary containing 50 mM Tris-HCl buffer (pH 7.4), 100 mM NaCl, and 3 mM calf thymus B-DNA. Inspection of Figure 7 reveals that both complexes exhibit stereoselectivity in their binding with B-DNA. We have also performed experiments on each complex separately, and the migration velocities and stereoselectivity results are identical to the simultaneous separation of the 1:1 mixture of the two complexes.[21] Based on measured values of electrophoretic mobilities, μ_e (using a neutral marker to correct for the electroosmotic flow component), both complexes migrate at significantly reduced velocities in the presence of DNA. The Ru^{2+} isomers show slightly greater retardation in μ_e than the Cr^{3+} isomers, suggestive of a slightly larger K_{DNA} value.

Significantly, the enantiomeric order of migration and thus net binding stereoselectivities (established by co-injections with samples of the Λ isomer) are *reversed* for the Cr^{3+} and Ru^{2+} complexes. For the case of $Ru(phen)_3^{2+}$ with B-DNA, the CE results in Figure 7 demonstrate preferential binding by the Δ isomer—a result consistent with earlier equilibrium dialysis data.[22,23] Although the binding interaction of $Ru(phen)_3^{2+}$ with DNA is dominated by electrostatic forces,[23] the observation of enantiomeric discrimination, coupled with recent thermodynamic

(21) This observation is not surprising, since for 1:1 mixture injections the two complexes will be electrophoretically separated from one another as soon as the voltage is applied, and therefore may be treated independently with respect to their DNA interaction as they travel down the capillary.

(22) Barton, J. K.; Danishefsky, A. T.; Goldberg, J. M. *J. Am. Chem. Soc.* **1984**, *106*, 2172−2176.

(23) Satyanarakyana, S.; Dabrowiak, J. C.; Chaires, J. B. *Biochemistry* **1992**, *31*, 9319−9324.

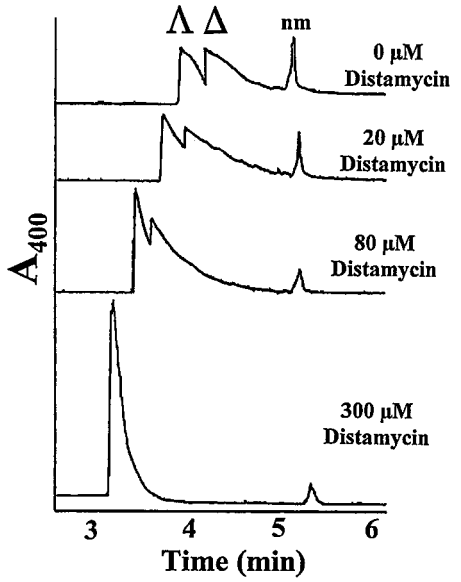

Figure 8. Successive electropherograms of *rac*-Ru(phen)$_3^{2+}$ (1 mM) in 50 mM Tris-HCl buffer, pH 7.4, containing 100 mM NaCl and 0.92 mM calf-thymus B-DNA in the presence of increasing concentrations of distamycin A. Electrophoretic field strength was 319 V/cm (50 μm i.d. *uncoated* capillary), using a run temperature of 35 °C. Detection was at $\lambda = 400$ nm (nm = neutral marker).

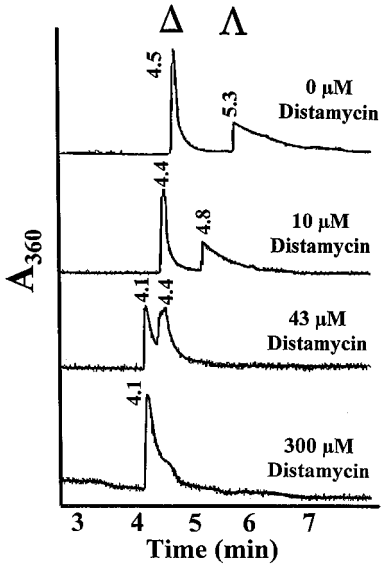

Figure 9. Successive electropherograms of *rac*-Cr(phen)$_3^{3+}$ (1.6 mM) in 50 mM Tris-HCl buffer, pH 7.4, containing 100 mM NaCl and 0.92 mM calf-thymus B-DNA in the presence of increasing concentrations of distamycin A. Electrophoretic field strength was 319 V/cm (50 μm i.d. *coated* capillary), using a run temperature of 35 °C. Detection was at $\lambda = 360$ nm.

data, argue that nonelectrostatic forces are not insignificant.[24] Several NMR studies on Ru(phen)$_3^{2+}$ employing oligonucleotides[25−28] indicate that these nonelectrostatic interactions occur primarily via surface binding in the *minor* groove near the AT base pair. Barton and co-workers[1a,25] and others[26−28] have proposed that this surface binding mode favors the Λ optical isomer. The Barton model assigns an additional binding mode with an unusually strong Δ preference to partial intercalation of a phenanthroline ligand in the *major* groove. Thus, although this latter mode makes only a small contribution to the overall binding constant, a net discrimination for the Δ isomer is observed. However, three more recent NMR studies suggest that the binding mode characterized by a strong Δ preference also occurs in the *minor* groove.[26−28]

That this latter interpretation is more applicable to the case of B-DNA comes from CE studies involving the addition of distamycin A to the *rac*-Ru(phen)$_3^{2+}$/B-DNA system. Distamycin A is a strongly AT selective *minor* groove binder with a large binding constant for B-DNA.[1b] Its presence in the capillary medium would therefore be expected to result in the release of *both* Ru(phen)$_3^{2+}$ enantiomers if the Λ and Δ isomers were both bound in the minor groove. In contrast, if the binding mode favoring the Δ isomer were associated with the major groove, then one anticipates that the addition of distamycin would lead to the experimental observation of an even greater net preference for Δ binding accompanying reduced overall binding. Our CE data for the *rac*-Ru(phen)$_3^{2+}$/B-DNA system in the presence of successively higher buffer concentrations of distamycin (varying from 0.02:1 to 0.3:1 mol distamycin/mol B-DNA) are shown in Figure 8.[29] It is evident that even low relative distamycin concentrations cause a significant reduction in Ru(phen)$_3^{2+}$ migration times (and increased mobilities). More importantly, reduced migration times are accompanied by the complete loss of enantiomeric discrimination, suggesting that the binding mode characterized by a strong Δ preference *also* occurs in the *minor* groove.

For the case of Cr(phen)$_3^{3+}$, a pertinent earlier study is the NMR investigation by Rehmann and Barton[30] on the oligonucleotide d(GTGCAC)$_2$ in the presence of Cr(phen)$_3^{3+}$. Their results were interpreted in terms of minor groove surface binding in which Λ isomer binding was favored. In this case they found only weak evidence for an additional binding mode favoring Δ isomer binding in the *major* groove. In a related NMR study involving Ru(phen)$_3^{2+}$ and Rh(phen)$_3^{3+}$,[25] Rehmann and Barton noted that increasing complex charge is an additional factor favoring surface binding over partial intercalation. Our observation (Figure 7) of net preferential binding by the Λ isomer of Cr(phen)$_3^{3+}$ is therefore not unexpected. We have also conducted distamycin CE studies for the Cr(phen)$_3^{3+}$/B-DNA system.[31] In the presence of increasing concentrations of distamycin in the buffer medium (Figure 9), a progressive loss of enantiomeric stereoselectivity is observed. This result suggests that both binding modes (including the very weak intercalative component) involve the minor groove.

Acknowledgment. Support of this research by the Research Corp., the NSF-REU Program, and the Duke Endowment is gratefully acknowledged.

IC980857L

(24) Kalsbeck, W. A.; Thorp, H. H. *Inorg. Chem.* **1994**, *33*, 3427−3429.
(25) Rehmann, J. P.; Barton, J. K. *Biochemistry* **1990**, *29*, 1701−1709.
(26) Norden, B.; Patel, N.; Hiort, C.; Graslund, A.; Kim, S. K. *Nucleosides Nucleotides* **1991**, *10*, 1991.
(27) Eriksson, M.; Leijon, M.; Hiort, C.; Norden, B.; Graslund, A. *Biochemistry* **1994**, *33*, 5031−5040.
(28) Collins, J. G.; Sleeman, A. D.; Aldrich-Wright, J. R.; Greguric, I.; Hambley, T. W. *Inorg. Chem.* **1998**, *37*, 3133−3141.
(29) The electrophoretic response of the neutral marker (nm) is shown for clarity for this uncoated capillary to demonstrate the reproducibility of electroosmotic flow. The longer migration time observed for Ru(phen)$_3^{2+}$ in Figure 7 compared with that for Ru(phen)$_3^{2+}$ in the absence of distamycin in Figure 8 is associated with the smaller electrophoretic field strength and higher DNA concentration used for the collection of the Figure 7 data.
(30) Rehmann, J. P.; Barton, J. K. *Biochemistry* **1990**, *29*, 1710−1717.
(31) A coated capillary was used for this Cr(phen)$_3^{3+}$ study to eliminate electroosmotic flow, thereby enhancing the separation observed between the Λ and Δ isomers relative to that observed in Figure 7.